ENGINEERING RESEARCH INSTITUTE
UNIVERSITY OF MICHIGAN
ANN ARBOR

GROWTH OF THE TURBULENT REGION AT THE LEADING EDGE OF RECTANGULAR OBSTACLES IN SHOCK WAVE DIFFRACTION

REPORT 51 - 2

ROBERT N. HOLLYER, JR.

RUSSELL E. DUFF

Supervised by

OTTO LAPORTE

January 18, 1951

THIS REPORT PUBLISHED

FOR

Armed Forces

Special Weapons Project

for

dissemination to

authorized agencies

TABLE OF SYMBOLS

$\xi = \frac{P_o}{P_1} = \frac{1}{S}$

a = local velocity of sound.

t = time measured in microseconds, where t = 0 when primary shock shock wave is at the leading edge of the model.

*D = distance from leading edge of model to leading edge of boundary layer.

M = Mach number behind primary shock.

*P_o = pressure ahead of primary shock

P_1 = pressure behind primary shock in the undistrubed flow.

$S = \frac{P_1}{P_o} = \frac{1}{\xi}$

*T = time for primary shock to travel 500 millimeters.

T = measured delay time of photograph.

T' = delay time to place the primary shock at the leading edge of the model.

U = flow velocity behind primary shock wave.

*X = length of turbulent or vortex region.

*Y = height of turbulent or vortex region.

*Z = distance from leading edge of the model to the center of the vortex.

* Measured quantities.

GROWTH OF THE TURBULENT REGION AT THE LEADING EDGE OF RECTANGULAR OBSTACLES IN SHOCK WAVE DIFFRACTION

I. INTRODUCTION

This report presents the results of an investigation of the growth of the vortex or turbulent region at the leading edge of a rectangular block following the passage of a shock wave over the block. The primary purpose of the study is to determine the dependence of the growth upon the various parameters of the problem, namely, model height, shock strength, and flow velocity. The length of the block is assumed to be infinite. A representative sequence of schlieren photographs of the phenomenon under investigation is included as Fig. 10.

II. EXPERIMENTAL PROCEDURE

The data were obtained in the University of Michigan 2-inch by 7-inch rectangular shock tube. The models used were 8-inch by 2-inch rectangular steel blocks of various heights placed on the floor of the tube (see Fig. 1). Both schlieren and shadow photography were used.

Table I contains the data for the three values of shock velocity used.

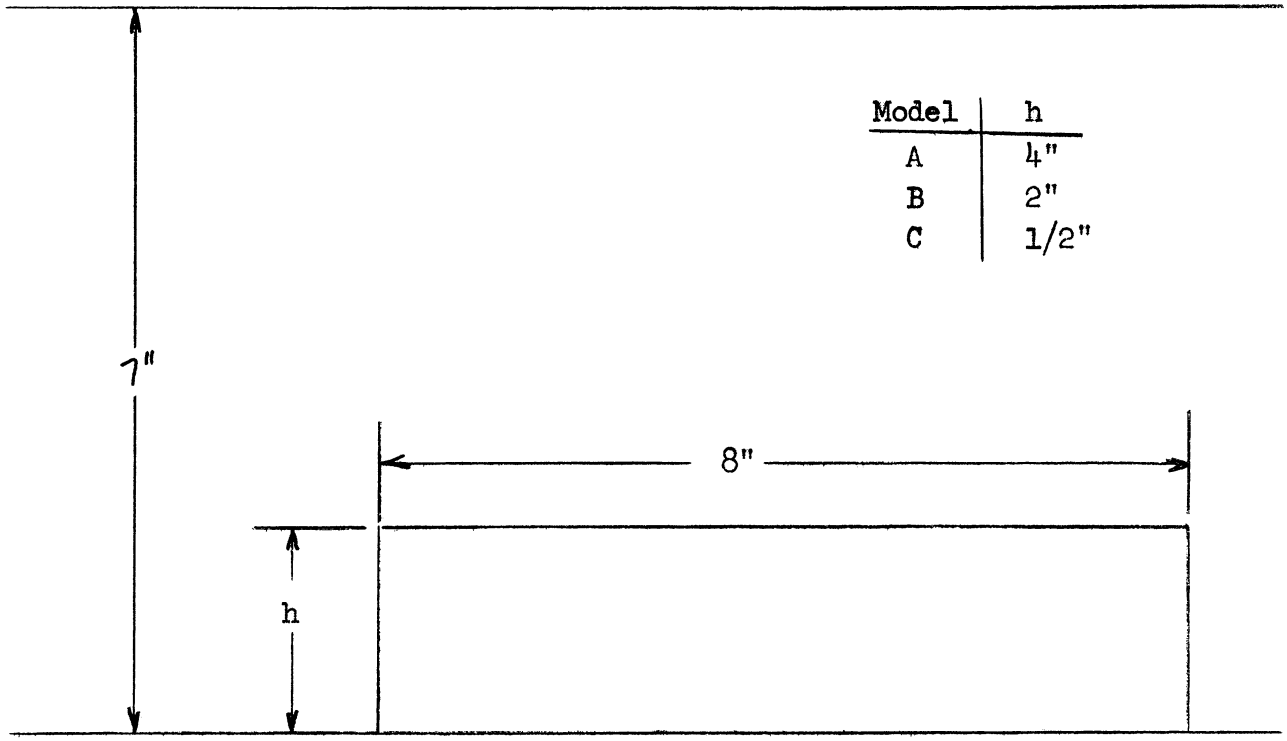

Fig. 1

TABLE I

Gas	V	P_o/P_1	P_1/P_o	U	M	a	$T_{correct}$
Air	0.4062	0.6916	1.446	0.0936	0.257	0.364	1231
N_2	0.4062	0.7005	1.427	0.0908	0.248	0.366	1231
Air	0.4482	0.5557	1.800	0.1524	0.403	0.378	1115
N_2	0.4482	0.5628	1.777	0.1494	0.395	0.378	1115
Air	0.5682	0.3332	3.001	0.2992	0.774	0.386	880
N_2	0.5682	0.3388	2.951	0.2963	0.717	0.413	880

(All velocities are in mm per μsec.)

Data for both air and nitrogen are tabulated. Nitrogen was employed for those cases in which a greater density of gas seemed desirable. It was necessary to use nitrogen instead of air to accomplish this because hydrogen was used in the compression chamber of the shock tube for these higher density shots. In some cases, a variation of density was used to alter the kinematic viscosity to determine the dependence of the phenomenon upon this parameter. In other cases, the density was increased to enhance the optical effects of the disturbance. This made it possible to extend the data to larger values of t than would have been possible with the use of air alone.

The parameters chosen as characteristic of the region under study are the length X and the height Y of the turbulent region, as illustrated in the following diagram.

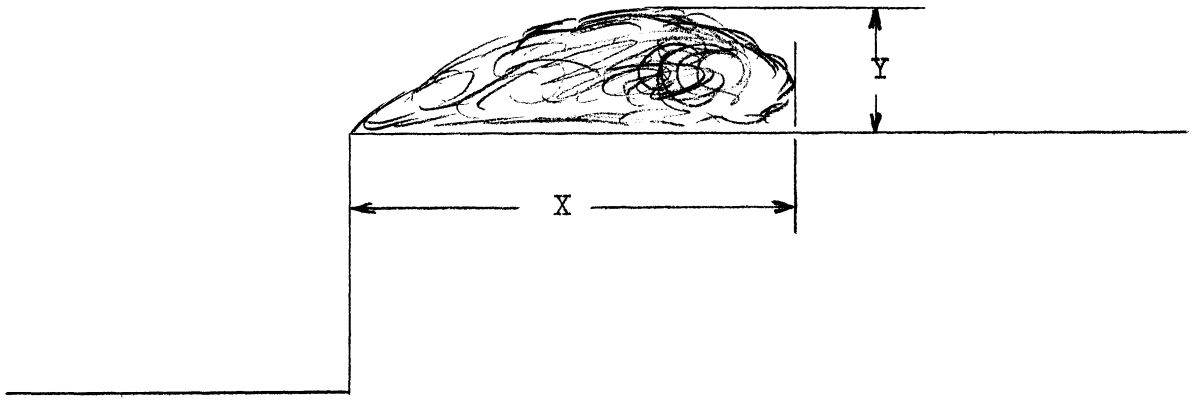

For the lower values of t, the boundary of the region is fairly well defined, but as t increases, this boundary becomes less distinct. In all cases the measurement was made to last observable disturbance of the smooth flow. The probable error of the measurements for the largest values of t should not be considered to be less than $\pm$ 3 mm. The errors are most probably in the negative direction, i.e., a low value of the variable is most probably reported.

In the case of the two lower values (S = 1.44, 1.8) the region under consideration begins as a fairly well-defined vortex which eventually disintegrates. While this vortex is visible, the motion of its center can be traced. This has been done where possible, and the distance from the leading edge of the block to the center of the vortex is included in the data as Z.

Shadowgraph pictures of the two lower values of shock strengths (none were taken at S = 3) show the boundary layer behind the disturbed region. The distance between the leading edge of the model and the beginning of this boundary layer is shown in the data as D. Because this point can be located with accuracy only for lower values of t and because of the uncertainty concerning the interpretation of the data obtained, it was felt that it would be unwise to consider it seriously in this report.

Except where otherwise indicated, the value of t associated with each photograph is obtained from the electronic control equipment, which simultaneously records on microsecond scalers the time, T, for the shock to travel 500 millimeters and the delay time, T*, of the photograph. From pictures containing the primary shock, the delay time, T', needed to place the shock wave at the leading edge of the model for a given shock velocity can be computed. For later photographs at this same shock velocity, the time, t, can then be obtained from the equation:

$$t = T^* - T'$$

Since it is not always possible to reproduce shock velocities exactly it is necessary to correct the value of T*, and thus t, to compensate for the

variations in the measured shock velocity. This is done by determining the value of T^* which would have been needed to place the primary shock in its actual position at the time the photograph was taken if the correct value of the shock velocity had been obtained. This corrected value of T^* is simply:

$$T^*(\text{corrected}) = T^*(\text{measured}) \frac{T(\text{corrected})}{T(\text{measured})}$$

Table II shows the values of T (corrected) used in this report and the maximum deviations from this value in addition to the percentage error introduced in the flow parameters for this maximum deviation.

TABLE II

P_1/P_o	T Corrected	Maximum Deviation	% Error in V	% Error in U	% Error in S
1.44	1231 μsec	4 μsec	0.3	2.0	0.8
1.8	1115	6	0.5	2.4	1.3
3.0	880	5	0.6	1.5	1.6

A consideration of the errors inherent in the integer time-measuring system used and the experimental techniques employed, gives a maximum error in t of no more than $\pm$ 5 microseconds. Since the errors due to all causes in the value of t are small by comparison to the errors in the measurements of the dimensions of the phenomenon, no corrections for shock velocity variations have been applied to the measured values of X, Y, Z, and D.

These procedures have been used in handling data presented in the past and, unless otherwise indicated, will be used in the future for reports prepared for the Armed Forces Special Weapons Project.

III. DISCUSSION OF THE DATA

In the early stages of this investigation it was noted that no significant difference existed between the data for the 2-inch block and the 4-inch block. Therefore, the major portion of the data has been collected for the 1/2-inch and 4-inch blocks. In addition, the fact that this phenomenon involves the viscosity of the gas, made it seem wise to vary the gas densities, and therefore the Reynolds number, in order to check any dependence of the data upon this parameter. The data obtained are shown in Tables III-VII.

Following standard procedure, the measured quantities, X and Y, were plotted against various parameters of the problem in an attempt to determine empirically the dependence upon such parameters. By far the most successful of these attempts was to plot X against the product of t and the flow velocity, U, behind the primary shock. These curves for the 4-inch, 2-inch, and 1/2-inch block are included as Figs. 2, 3, and 4. A composite curve of all values of X for the three different blocks is shown in Fig. 5. The curve of Y versus Ut for the 4-inch block is shown in Fig. 6. Figs. 7 and 8 are curves of Y versus Ut for the 2-inch and 1/2-inch block, respectively, while the composite curve of Y versus Ut for all models is shown in Fig. 9. The values of U used for these curves are those given in Table I. No corrections have been applied for variations of the actual flow velocity from the ideal values listed in that table.

The following features of these curves are of particular importance:

(a) The curves of Figs. 2, 3, 4, 6, 7, and 8 indicate that for a given block the size of the turbulent region is a function of the product of the flow velocity, U, and the time, t, and not of U or t separately. This

means that we have obtained the empirical result that:

$$X = X(Ut),$$

$$Y = Y(Ut).$$

(b) The curves of X versus Ut for a given model are straight lines within the experimental error of the points. This is a rather surprising result, first, because it indicates that the change from vortex flow to apparently uniform turbulence does not effect the growth of the disturbed region, and secondly, it indicates an extremely weak dependence of the growth of X upon the presence of the upper wall of the shock tube. The approximate points at which the conversion from vortex flow to turbulence takes place can be obtained by noting those values of Ut in the data to which no value of the parameter, Z, has been assigned.

(c) The slope of the curve X versus Ut is almost identical for all blocks (see Fig. 5). The plotted points indicate that the curve for the 1/2-inch block is slightly lower than those for the 2- and 4-inch block. It is difficult to make any quantitative statement, however, because of several experimental factors. First, since the turbulence in the region under discussion is much less pronounced in the case of the 1/2-inch block, the measurement errors here would tend to lower the curve below those of the higher blocks. Secondly, the effect of the upper wall of the shock tube is considerably less for this model. The first reflected shock arrives at the top of the model at a value of Ut about twice the value for the corresponding flow using the 4-inch block. Furthermore, since this shock is approximately cylindrical, it will be weaker than that for the 4-inch case.

(d) The curve Y versus Ut (Fig. 6) is a straight line for the 1/2-inch block, while it appears to be approaching some fixed value for the two higher models. We cannot quantitatively explain this result, but again the

effect of the top wall of the tube seems to be the most promising qualitative explanation. The reflection from the top of the tube interferes with the turbulent region at about 40, 60, and 100 mm Ut for shock strengths S = 1.44, 1.8, and 3.0, respectively, for the 4-inch block, and at about twice these values for the 1/2-inch block. It seems logical to expect the effect of the top wall to produce greater changes in vertical velocity components for the large blocks than for the small block.

(e) Contrary to the situation we found for the X versus Ut curves that the slopes are not equal for all block in the case of Y versus Ut. This result is not unexpected, since the effect of the variable height of the models is naturally stronger for vertical measurement. There are not sufficient data, nor is the experimental accuracy good enough, to arrive at any reliable dependence of the slope on block height. The slopes for the 2- and 4-inch block seem to be almost equal, while that for the 1/2-inch block is approximately one half of these. In addition, the slope for S = 3.0 appears to be a bit lower than that for the other values of S. This latter observation is complicated by the fact that the region above the turbulence is clearly supersonic, since a cluster of shock waves can be observed in all photographs (see Fig. 11). The presence of these extra disturbances makes the measurement of Y extremely difficult. Because of this and because of the small number of points plotted, nothing reliable can be deduced from this observation.

Conclusions

Within the range of the variables studied in this investigation, the following conclusions seem to be valid:

(a) The curve of X versus Ut is a straight line whose slope is the same for all block heights, shock strengths, and gas densities.

(b) The curve of Y versus Ut is a straight line whose slope is independent of shock strength and gas density but is some undetermined function of block height. More data must be obtained if this dependence is to be empirically determined.

(c) There is no observable effect upon the growth as the flow in the region under question changes from a vortex flow to a turbulent flow.

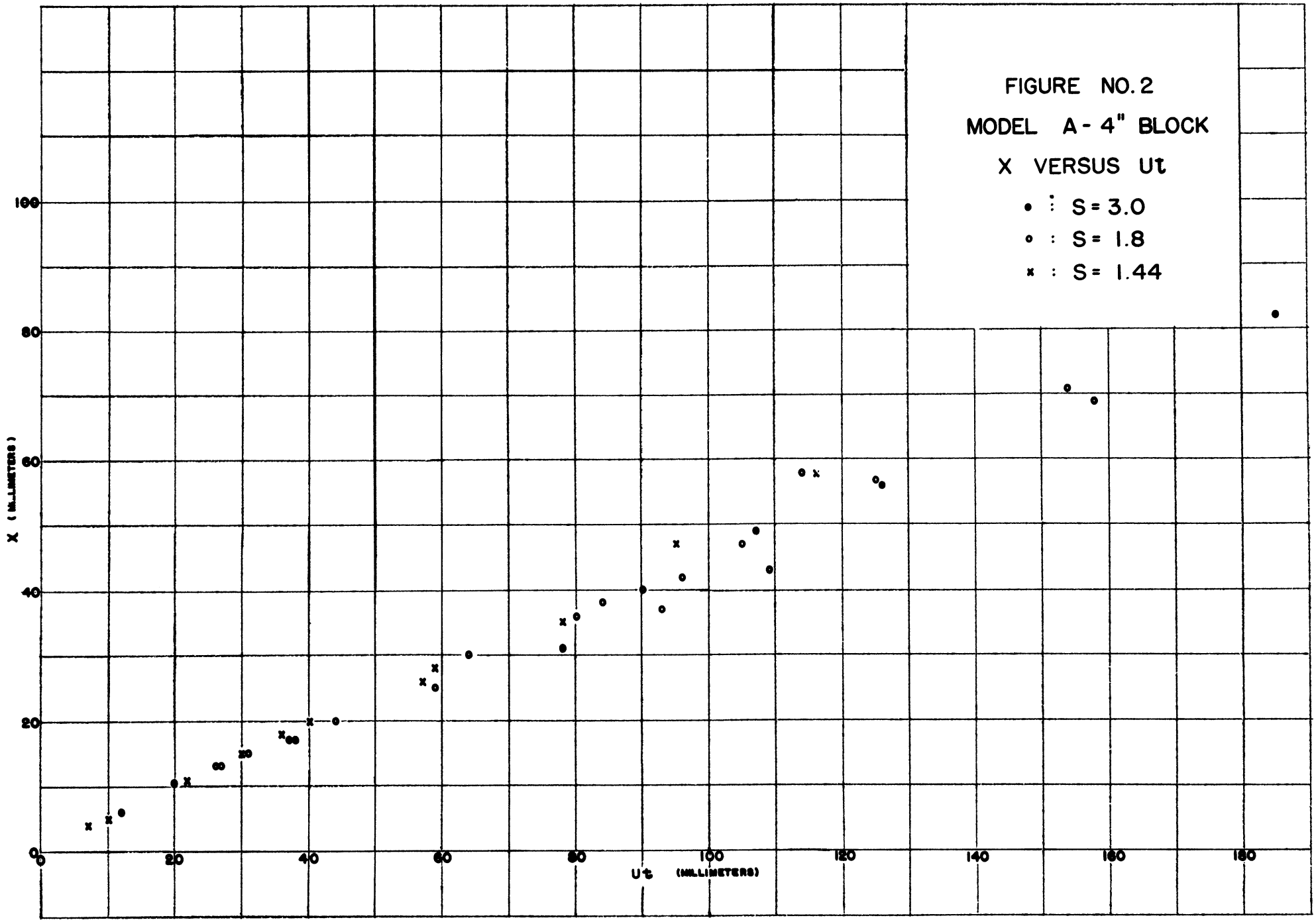
FIGURE NO. 2
MODEL A - 4" BLOCK
X VERSUS Ut
• : S = 3.0
o : S = 1.8
x : S = 1.44
X (MILLIMETERS)
Ut (MILLIMETERS)
0
20
40
60
80
100
120
140
160
180

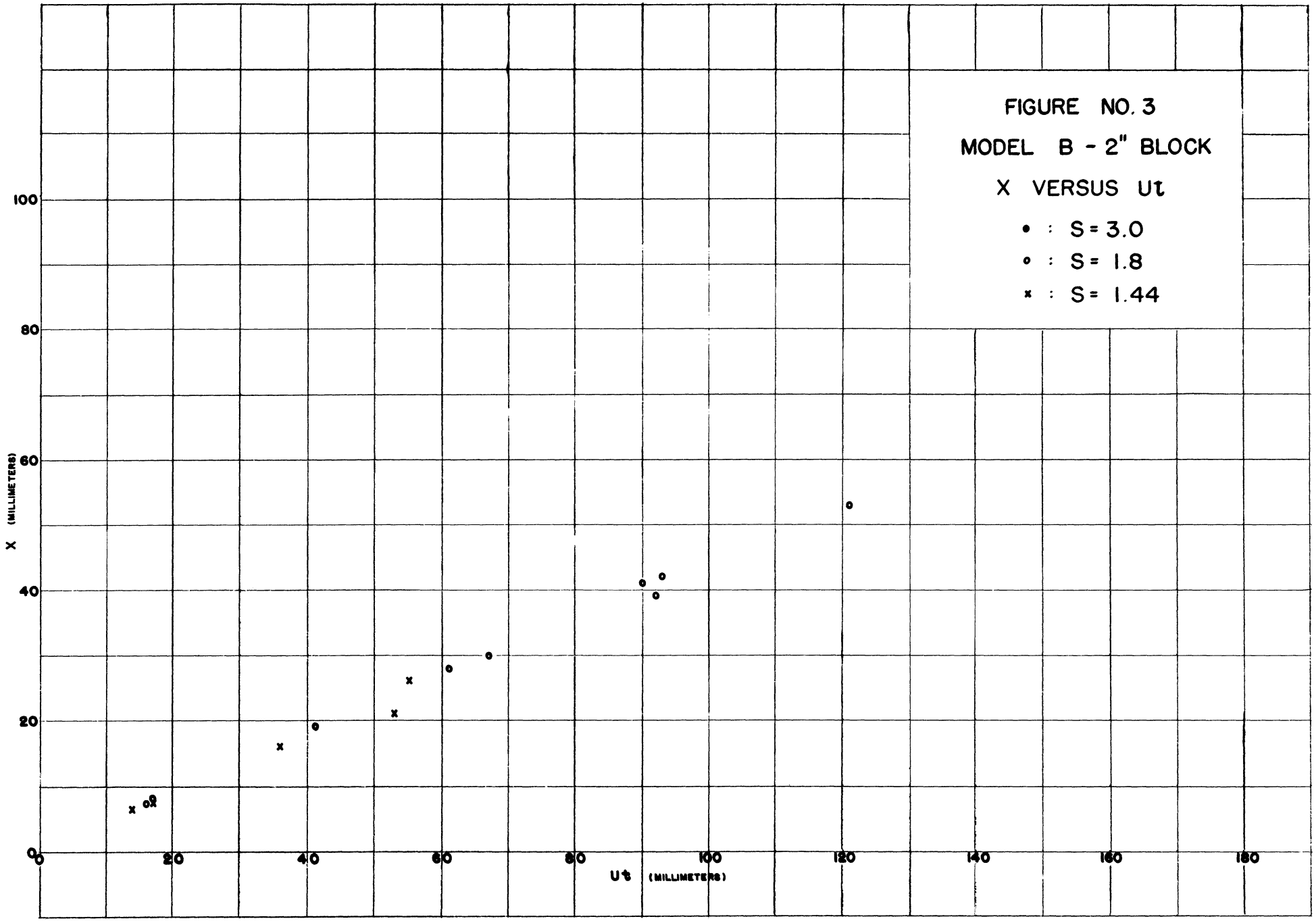
FIGURE NO. 3
MODEL B - 2" BLOCK
X VERSUS Ut
• : S = 3.0
o : S = 1.8
× : S = 1.44
X (MILLIMETERS)
Ut (MILLIMETERS)
0
20
40
60
80
100
120
140
160
180

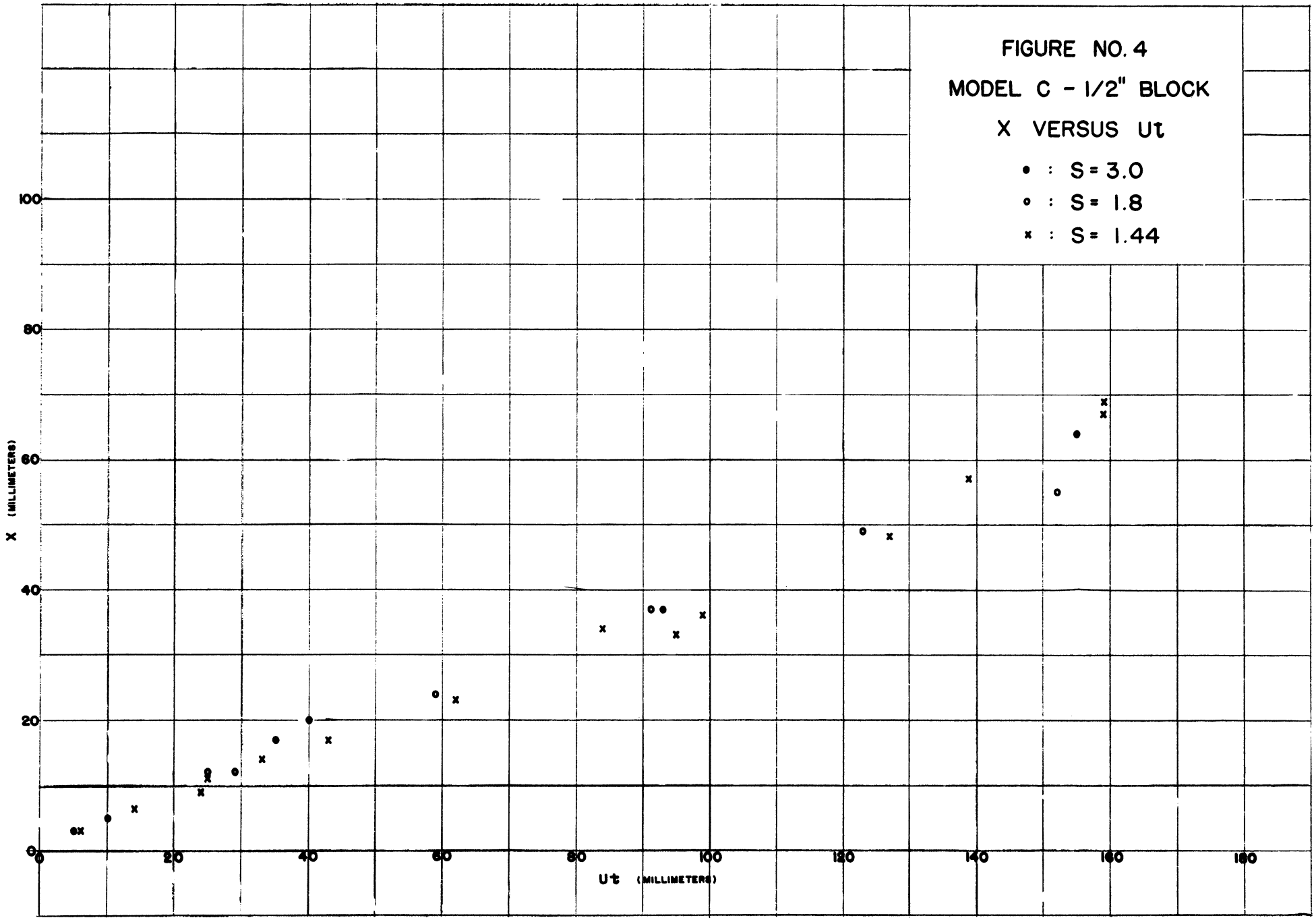
FIGURE NO. 4
MODEL C - 1/2" BLOCK
X VERSUS Ut
• : S = 3.0
o : S = 1.8
× : S = 1.44
X (MILLIMETERS)
Ut (MILLIMETERS)
0
20
40
60
80
100
120
140
160
180

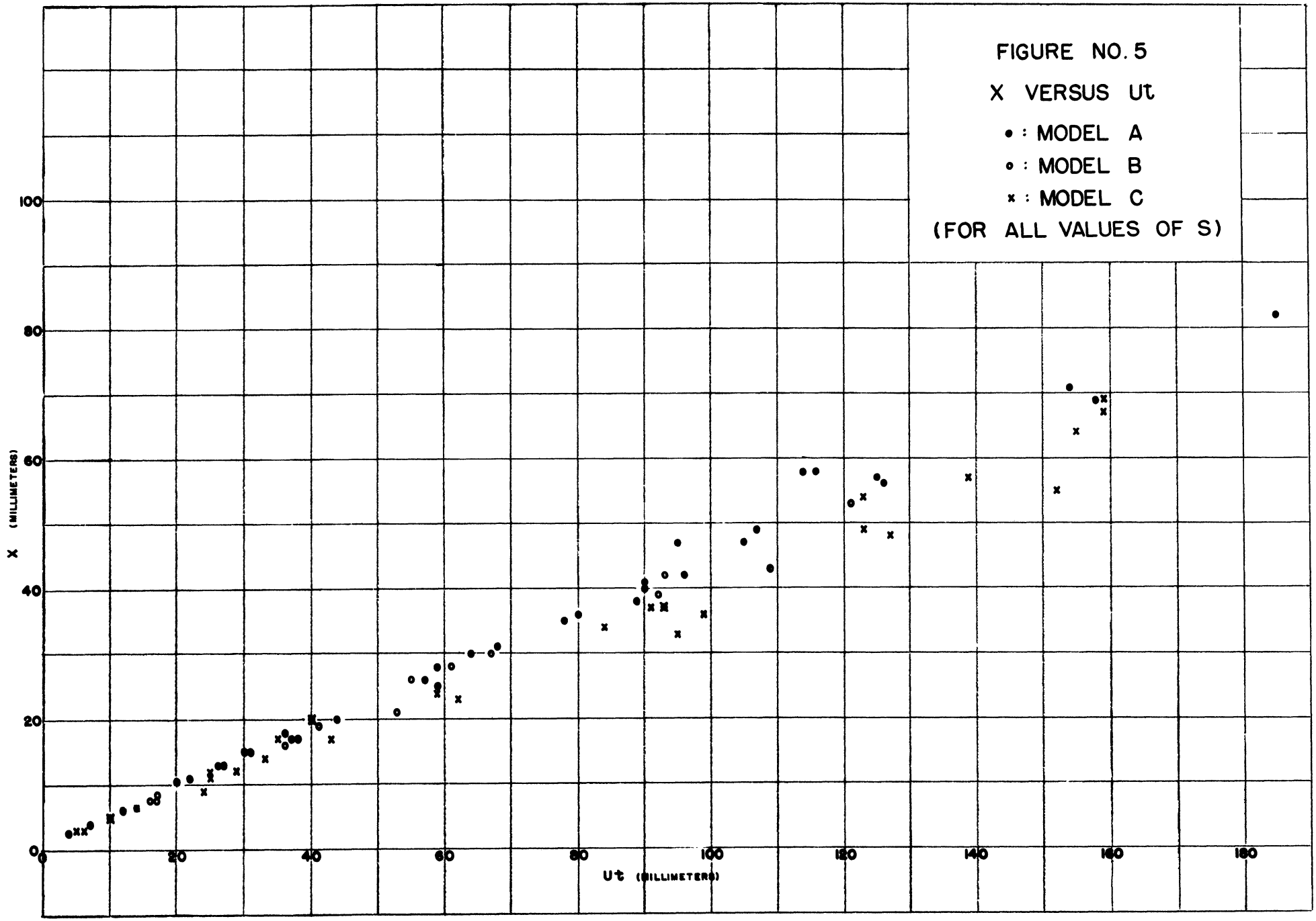
FIGURE NO. 5
X VERSUS Ut
• : MODEL A
o : MODEL B
× : MODEL C
(FOR ALL VALUES OF S)
X (MILLIMETERS)
Ut (MILLIMETERS)
0
20
40
60
80
100
120
140
160
180

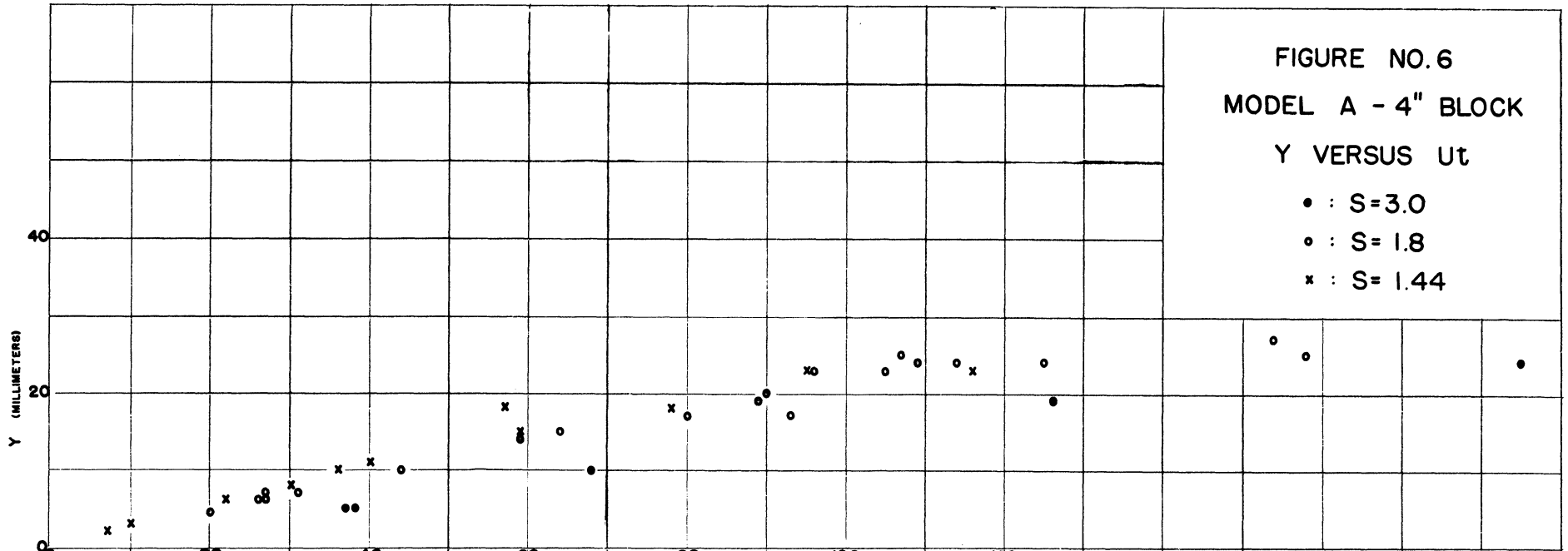

FIGURE NO. 6

MODEL A - 4" BLOCK

Y VERSUS Ut

• : S=3.0

o : S= 1.8

x : S= 1.44

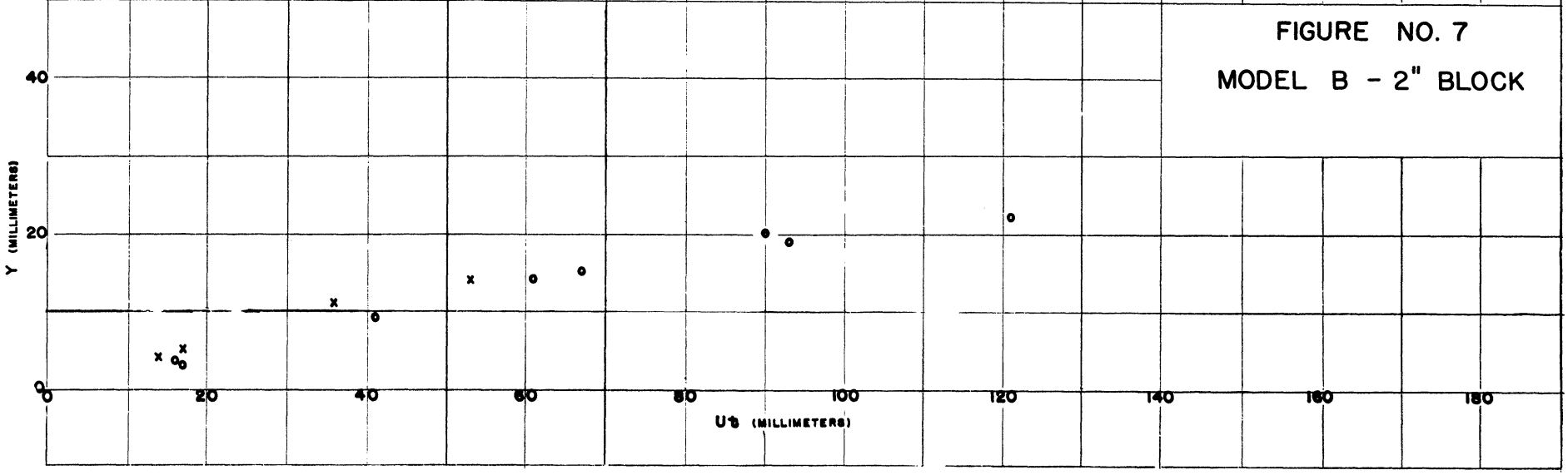

FIGURE NO. 7

MODEL B - 2" BLOCK

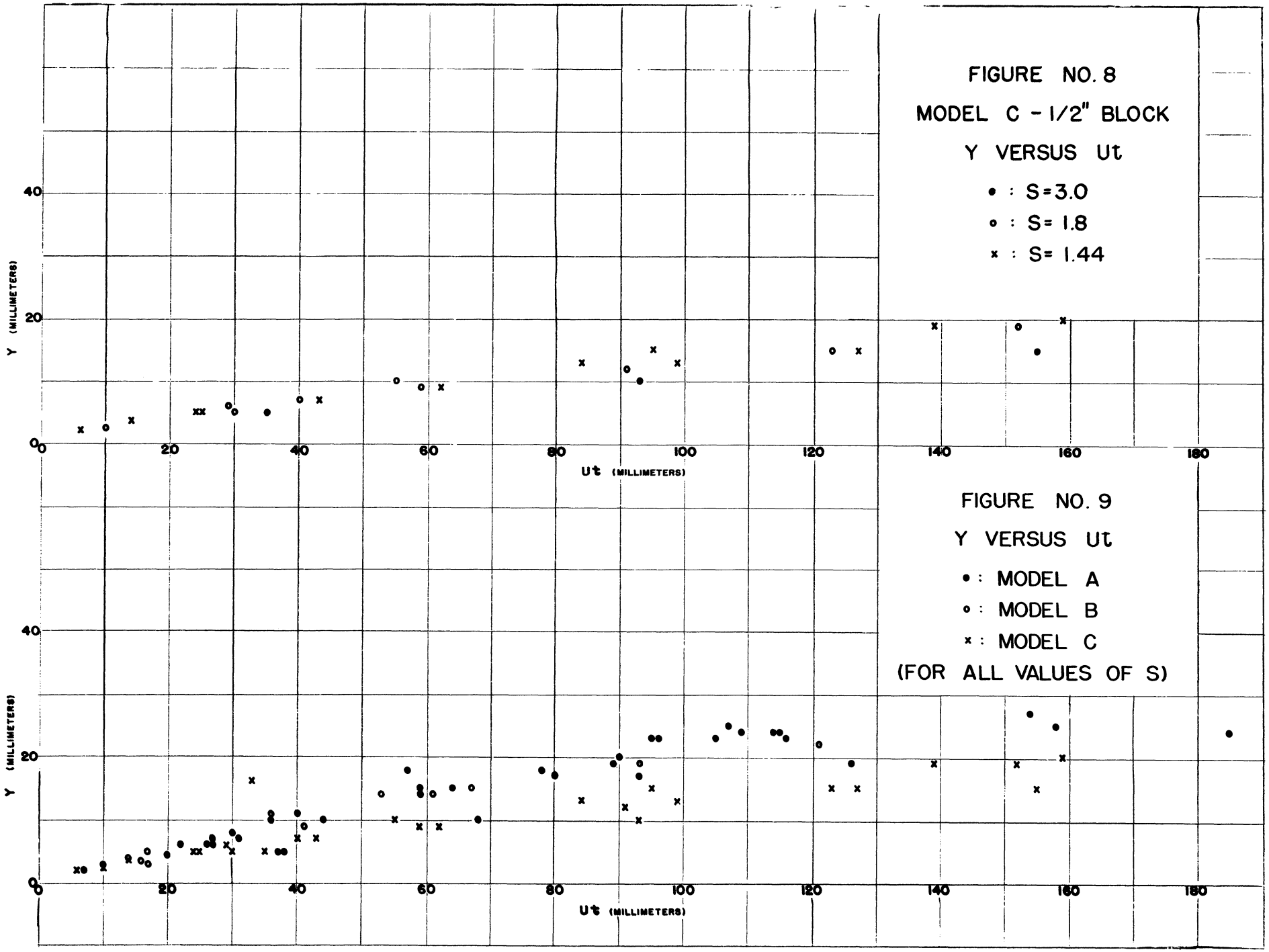

FIGURE NO. 8

MODEL C - 1/2" BLOCK

Y VERSUS Ut

• : S=3.0

o : S= 1.8

× : S= 1.44

FIGURE NO. 9

Y VERSUS Ut

• : MODEL A

o : MODEL B

× : MODEL C

(FOR ALL VALUES OF S)

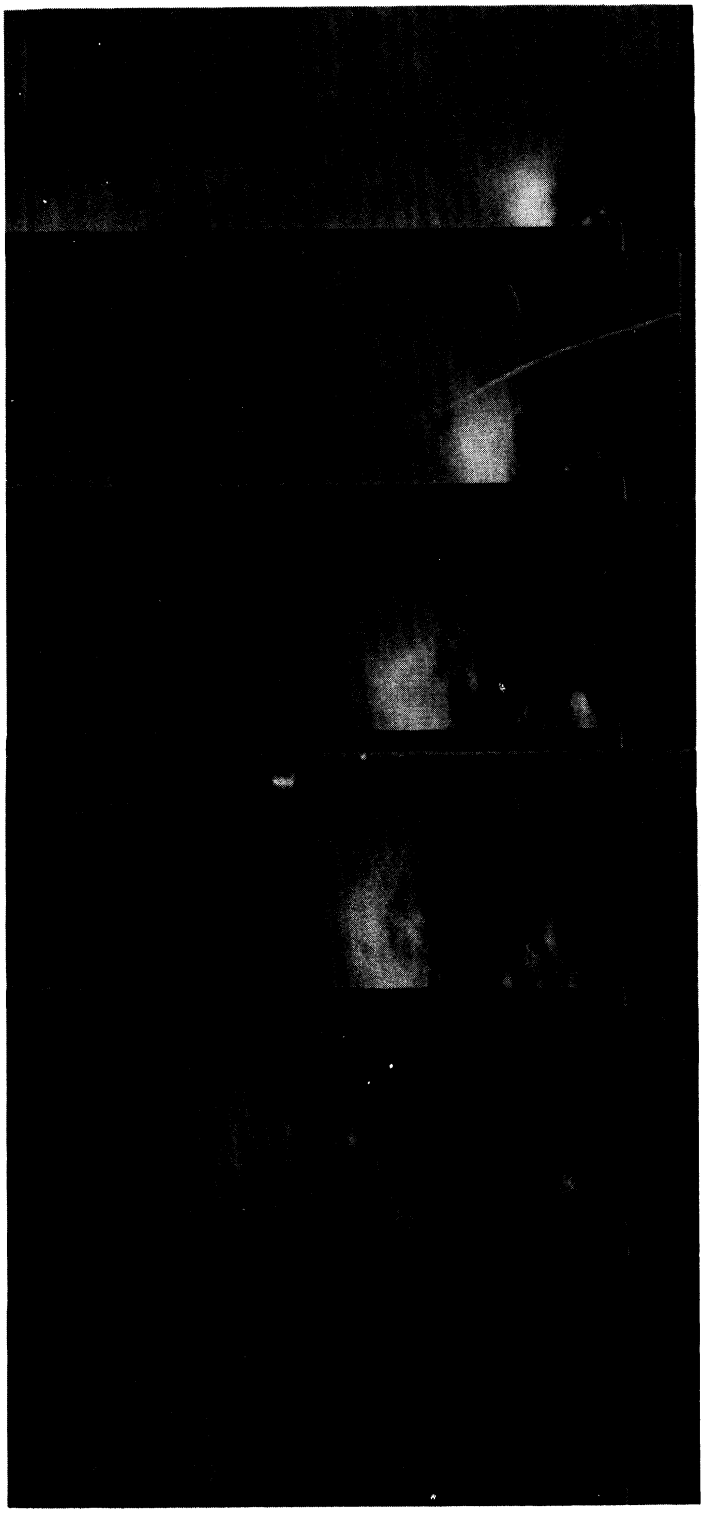

t = 205 microseconds

t = 389

t = 609

t = 716

t = 1034

t = 1428

Fig. 10

S = 1.8, 4-inch block

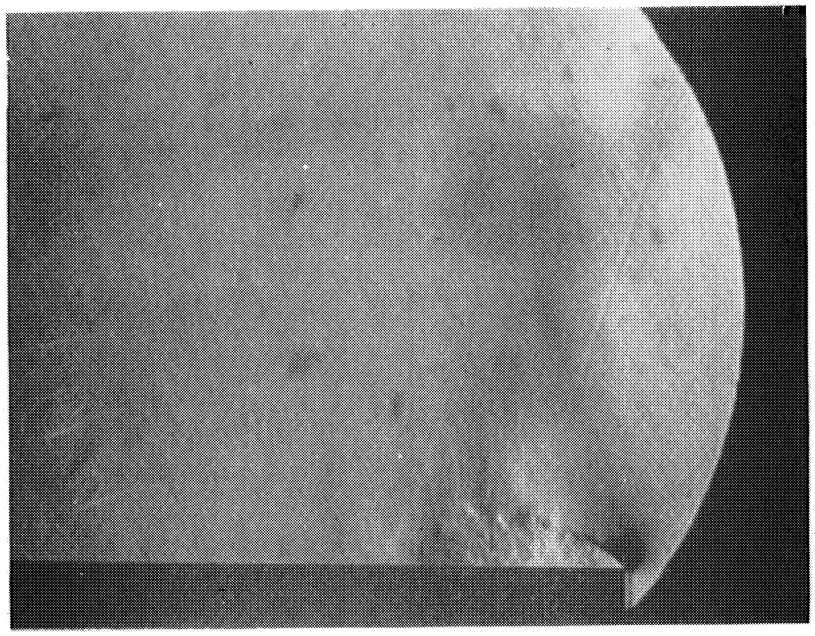

Fig. 11

S = 3.0, t = 230, 4-inch block

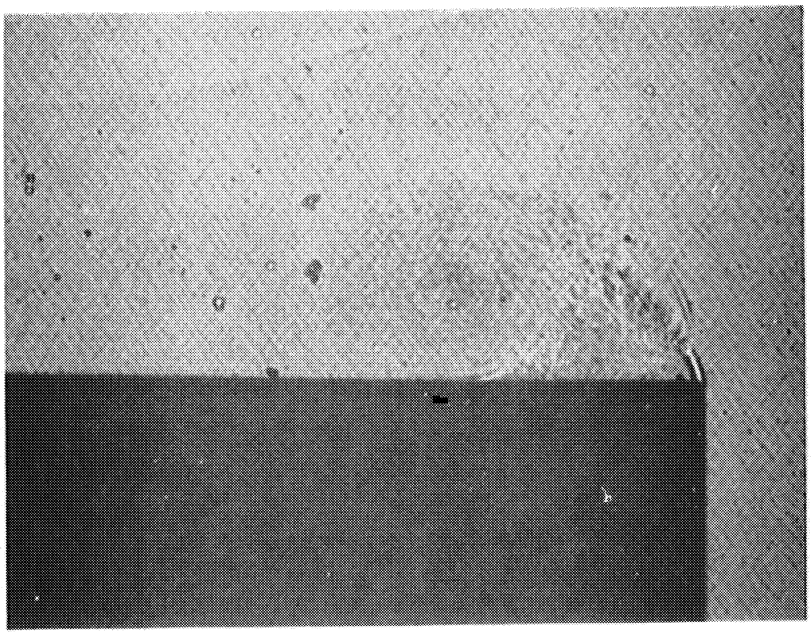

Fig. 12

Shadowgraph, S = 1.44, t = 388, 4-inch block

TABLE III

S = 1.44 Schlieren

Model	t	P_o	Gas	Film	X	Y	Z	Ut
	(sec)	(mm of Hg)		No.	(mm)	(mm)	(mm)	(mm)
A**	77*	475	N_2	160	4	2	2	7
A	245	475	N_2	161	11	6	6	22
A	444	475	N_2	162	20	11	12	40
A	647	475	N_2	163	28	15	18	59
A	860	475	N_2	164	35	18	20	78
A	1050	475	N_2	165	47	23	--	95
A	1283	475	N_2	166	58	23	--	116
C**	71*	475	N_2	191	3	2	2	6
C	278	475	N_2	192	11	5	--	25
C	476	475	N_2	193	17	7	--	43
C	680	475	N_2	194	23	9	--	62
C	902	760	Air	243	34	13	--	84
C	1011	760	Air	240	33	15	--	95
C	1063	760	Air	244	36	13	--	99
C	1359	760	Air	241	48	15	--	127
C	1694	760	Air	242	69	20	--	159
C	1482	760	Air	245	57	19	--	139
C	1694	760	Air	246	67	--	--	159

* For these photographs t was computed from measurements of the position of the primary shock.

** Model A = 4-inch block
Model B = 2-inch block
Model C = 1/2-inch block

TABLE V

S = 1.8 Schlieren

Model	t	P_o	Gas	Film	X	Y	Z	Ut
	(sec)	(mm of Hg)		No.	(mm)	(mm)	(mm)	(mm)
A	171	760	N_2	182	13	6	8	26
A	177	760	N_2	181	13	7	8	27
A	179	200	N_2	178	13	6	7	27
A	205	200	Air	135	15	7	10	31
A	389	200	Air	132	25	14	17	59
A	593	760	N_2	183	38	19	22	89
A	605	350	N_2	177	40	20	22	90
A	609	200	Air	136	37	17	25	93
A	645	760	N_2	184	42	23	27	96
A	702	350	N_2	176	47	23	--	105
A	716	200	Air	139	43	24	30	109
A	717	760	N_2	185	49	25	--	107
A	764	200	N_2	179	58	24	--	114
A	820	200	Air	137	57	24	--	125
A	1028	760	N_2	186	71	27	--	154
A	1034	200	Air	138	69	25	--	158
A	1428	350	N_2	140	94	26	--	213
B	401	200	Air	106	28	14	17	61
B	592	200	Air	109	41	20	27	90
B	611	200	Air	105	42	19	29	93
B	794	200	Air	108	53	22	--	121
C	191*	200	Air	126	12	6	7	29
C	389	200	Air	125	24	9	14	59
C	599	200	Air	124	37	12	24	91
C	805	200	Air	123	49	15	--	123
C	1000	200	Air	127	55	19	--	152

TABLE VI

S = 1.8 Shadowgraph

Model	t	P_o	Gas	Plate	X	Y	D	Ut
	(sec)	(mm of Hg)		No.	(mm)	(mm)	(mm)	(mm)
A	27*	200	Air	1013	2.5	--	--	4
A	136*	200	Air	1015	10.5	4.5	--	20
A	291	200	Air	1017	20	10	16	44
A	421	200	Air	1014	30	15	21	64
A	524	200	Air	1018A	36	17	26	80
A	693	200	Air	1018B	--	--	35	106
B	107*	200	Air	1036A	7.5	3.5	7	16
B	114*	200	Air	1039A	8.5	3	6	17
B	272	200	Air	1036B	19	9	14	41
B	438	200	Air	1037A	30	15	22	67
B	605	200	Air	1037B	39	--	30	92
B	625	200	Air	1039B	--	--	31	95
C	65*	200	Air	1043A	5	2.5	--	10
C	163*	200	Air	1043B	12	5	11	25
C	263	200	Air	1044A	20	7	18	40
C	363	200	Air	1044B	--	10	23	55
C	561	200	Air	1045A	--	--	32	85
C	762	200	Air	1045B	--	--	45	116

TABLE VII

S = 3.0 Schlieren

Model	t	P_o	Gas	Film	X	Y	Z	Ut
	(sec)	(mm of Hg)		No.	(mm)	(mm)	(mm)	(mm)
A	40*	165	N_2	169	6	--	2	12
A	124*	106	N_2	175	17	5	--	37
A	128	165	N_2	174	17	5	--	38
A	230	165	N_2	170	31	10	--	68
A	425	165	N_2	171	56	19	--	126
A	626	165	N_2	172	82	24	--	185
A	824	165	N_2	173	114	31	--	244
C	18*	165	N_2	197	3	--	1.5	5
C	117*	165	N_2	198	17	5	--	35
C	315	165	N_2	199	37	10	--	93
C	522	165	N_2	200	64	15	--	155
C	710	165	N_2	201	107	20	--	210
C	921	165	N_2	202	>109	20	--	273